



Stepwise progression of invasive mucinous adenocarcinoma based on radiological and biological characteristics

Eisuke Goto^a, Kazuya Takamochi^{a,*}, Satsuki Kishikawa^b, Takuo Hayashi^b, Takuya Ueda^a, Aritoshi Hattori^a, Mariko Fukui^a, Takeshi Matsunaga^a, Kenji Suzuki^a, & on behalf of the Tokyo Metropolitan Innovative Oncology Research Group (TMIG)

^a Department of General Thoracic Surgery, Juntendo University School of Medicine, Japan

^b Department of Human Pathology, Juntendo University School of Medicine, Japan

ARTICLE INFO

Keywords:

Invasive mucinous lung adenocarcinoma
Genetic alternation
MUC1
MUC6

ABSTRACT

Introduction: Invasive mucinous lung adenocarcinoma (IMA) has unique radiological findings and pathological characteristics. IMA is classified into solitary and pneumonic types; however, it is unclear whether these are biologically identical.

Methods: A single-center retrospective analysis was performed for 70 IMA patients (solitary type [n = 38] and pneumonic type [n = 32]) who underwent pulmonary resection between January 2010 and December 2018. We compared clinical and biological characteristics between the two types.

Results: The frequencies of genetic alternations such as EGFR, KRAS, BRAF, GNAS, ERBB2, TP53, NRG1, and MET were not different. Immunohistochemically, expression of MUC1 was significantly more common in the pneumonic type (5.0% versus 20.0%, p = 0.01) and diffuse MUC6 positive in the solitary type (39.0% versus 13.0%, p = 0.02). We further classified solitary types into those with or without ground-glass opacity (GGO) and pneumonic types into those with or without crazy-paving appearance (CPA), and evaluated their surgical outcomes. Five-year overall survival and relapse free survival rates were 95.8%/86.6%, 64.3%/70.7%, 74.6%/68.9%, and 50.0%/28.6% in patients with solitary type with GGO, solitary type without GGO, pneumonic type without CPA, and pneumonic type with CPA, respectively.

Conclusions: There were no differences in genetic alternations; however, mucin expression pattern was different. Surgical outcomes were different according to the presence of GGO in the solitary type and the presence of CPA in the pneumonic type. These findings suggested a stepwise progression from solitary to pneumonic IMA.

1. Introduction

Invasive mucinous lung adenocarcinoma (IMA), formerly known as mucinous bronchoalveolar carcinoma (BAC), is a subtype of lung adenocarcinoma and accounts for approximately 2–5% of lung adenocarcinoma [1,2]. In 2015, the World Health Organization (WHO) updated its classification, and IMA was classified as an invasive adenocarcinoma subtype [1,3].

Pathologically, tumor cells of IMA have a goblet or columnar cell morphologic pattern with abundant intracytoplasmic mucins [1,2]. IMA

exhibits different genotypic features relative to non-mucinous adenocarcinoma as EGFR mutations are rare and KRAS mutations are frequent in IMA, whereas in non-mucinous adenocarcinoma, EGFR mutations are frequent and KRAS mutations are rare [4–7]. We have recently reported that mucin expression pattern was closely related to surgical outcomes in IMA, and IMA with diffusely expressing MUC6 (expression of MUC6 ≥ 90% of tumor cells) had significantly favorable outcomes [8]. Yamanoi et al. also reported that MUC6 expression should be clinically checked as a favorable prognostic marker in IMA [9].

Radiologically, IMA is classified into two types: solitary and

Abbreviations: IMA, Invasive mucinous lung adenocarcinoma; BAC, Mucinous bronchoalveolar carcinoma; WHO, World Health Organization; CT, Computed tomography; PET, Positron emission tomography; FDG, ¹⁸F-fluorodeoxyglucose; GGO, Ground glass opacity; CPA, Crazy-paving appearance; OS, Overall survival; RFS, Relapse-free survival.

* Corresponding author at: Department of General Thoracic Surgery, Juntendo University School of Medicine, 1-3, Hongo 3-chome, Bunkyo-ku, Tokyo, 113-8431, Japan.

E-mail address: ktakamo@juntendo.ac.jp (K. Takamochi).

<https://doi.org/10.1016/j.lungcan.2023.107348>

Received 27 May 2023; Received in revised form 9 August 2023; Accepted 17 August 2023

Available online 20 August 2023

0169-5002/© 2023 Elsevier B.V. All rights reserved.

pneumonic, and the prognosis of the pneumonic type is worse than that of the solitary type [10–13]. However, it is unclear whether solitary type and pneumonic type IMA are biologically identical or not. IMA have a variety of radiological characteristics, such as airspace opacities, including both consolidation and ground-glass opacity (GGO), solid nodules, and mimicking infectious pneumonia [14]. In addition, several investigators reported that IMA has a unique radiological characteristic, the crazy-paving appearance (CPA) [15]. CPA was defined as scattered or diffuse ground-glass attenuation with superimposed interlobular septal thickening and intralobular lines on a CT scan [16], and it was known to be found in other diseases such as alveolar proteinosis and carcinomatous lymphangiosis [15], but, the clinical significance of CPA in IMA was unknown.

The aim of this study was to clarify the differences in radiological and biological characteristics between solitary type and pneumonic type IMA.

2. Materials and Methods

2.1. Study population

Between January 2010 and December 2018, 2213 patients underwent lung resection for adenocarcinoma at Juntendo University School of Medicine. Among these patients, 70 (3.2%) were diagnosed with IMA. This cohort is the same as that used in our previous report [8], and we extended the follow-up period to February 2022 in this study. Approval for this study was obtained from the Ethics Committee of Juntendo University School of Medicine (no. E22-0111; May 25, 2022).

2.2. Evaluation of clinical features and surgical policy

The clinical characteristics of patients, such as age, sex, smoking history, clinical stage, and mode of surgery were reviewed from the electronic medical records. For all patients, a thin-section computed tomography (CT) scan was performed within one month prior to surgery. The lung was photographed with a window level of -500 to -700 H and a window depth of 1000 to 2000 H as the “lung window,” and a window level of 30 to 60 H and a window depth of 350 to 600 H as the “mediastinal window.” The preoperative CT scan findings, such as total tumor size, presence of GGO component, presence of CPA component, solitary type, or pneumonic type were retrospectively reviewed by the three authors (EG, KT, and TU). Multiple lesions were defined as having one or more lesions larger than 5 mm in size other than the primary lesion. Solitary type IMA was defined as a solitary nodule or mass showing a round shape, and pneumonic type IMA was defined as a consolidation with an irregular margin (Fig. 1). Solitary type IMA was further classified into with or without the GGO component (Fig. 1A, B), and pneumonic type IMA was classified into with or without the CPA (Fig. 1D, C). Fifty-four patients (76%) underwent preoperative positron emission tomography (PET) using ^{18}F -fluorodeoxyglucose (FDG), and the maximum standardized uptake values (SUVmax) of the tumors were evaluated. After surgery, all patients underwent CT screening every 6 to 12 months. If any symptom or sign of recurrence, such as elevation of the tumor marker was observed, further radiological evaluation was added.

2.3. Pathological evaluation, genetic alterations, and immunohistochemistry

IMA was diagnosed according to the rules of the most recent WHO classification [2]. Analyses of genetic alterations and mucin expression were previously performed for all tumors [8]. In brief, EGFR and KRAS mutations were analyzed using the peptide nucleic acid-locked nucleic acid polymerase chain reaction (PCR) clamp method [17] and the peptide nucleic acid-mediated PCR clamping method [17], respectively, and TP53 and GNAS mutations were analyzed using PCR followed by direct sequencing [18]. Samples without EGFR/KRAS mutations were

subsequently analyzed by next-generation sequencing (NGS) including whole-exome sequencing and whole-transcriptome sequencing, as previously described [19], or targeted sequencing. Immunohistochemical examinations were performed using antibodies against MUC1 (Ma695, Leica Biosystems, Wetzlar, Germany), MUC4 (8G7, Santa Cruz Biotechnology, Dallas, TX, USA), MUC5AC (CLH2, Abcam, Cambridge, United Kingdom), and MUC6 (MUC6/916, Abcam). For the immunohistochemical analyses of MUC1, MUC4, MUC5AC, and MUC6, immunoreactivity was semi-quantitatively categorized as negative ($<10\%$ of tumor cells stained), positive ($\geq 10\%$ of tumor cells stained), or diffuse positive ($\geq 90\%$ of tumor cells stained).

2.4. Statistics analysis

Two category comparisons were performed using the chi-square test or Fisher's exact test, and numeric variables between the groups were compared by the Mann-Whitney U test. Overall survival (OS) and relapse-free survival (RFS) curves were plotted according to the Kaplan-Meier method and compared using the log-rank test in a univariate analysis. The date of surgical resection was set as the starting point, and censor was the last date of follow-up. The date of death was set as the event for OS, and the dates of death and relapse were set as the events for RFS. P -values < 0.05 were considered statistically significant.

3. Results

3.1. Classification of IMA

IMA was classified into solitary type ($N = 38$) and pneumonic type ($N = 32$) based on CT scan findings. We classified solitary type IMA into with GGO (Fig. 1A, $N = 24$) or without GGO (Fig. 1B, $N = 14$), and pneumonic type into without CPA (Fig. 1C, $N = 18$) or with CPA (Fig. 1D, $N = 14$). Representative histological findings of four types of IMA are shown in Fig. 2. Tumor cells had a goblet or columnar cell morphologic pattern with abundant intracytoplasmic mucins. Solitary type with GGO still had surrounding air space structures (Fig. 2A), while solitary type without GGO showed mucus filling in the air space (Fig. 2B). There was no histological difference between the solitary type without GGO (Fig. 2B) and the pneumonic type without CPA (Fig. 2C). Pneumonic type with CPA showed filling of the alveoli by abundant mucus, remaining air space, and honeycombing with thickening of the intralobular septa (Fig. 2D).

3.2. Clinical and biological characteristics of solitary type and pneumonic type IMA

The comparison of clinical and biological characteristics between solitary type IMA and pneumonic type IMA is summarized in Table 1. Age, sex, and smoking status were not significantly different between the two types. All solitary types were clinical stage I, while more than half of pneumonic types were stage II or more (52%). The surgical mode and extent of lymph node dissection were not different between the two types. Total tumor size was larger in the pneumonic type than that in the solitary type ($p < 0.01$), and the SUVmax of the tumor in the pneumonic type was significantly higher than that in the solitary type ($p < 0.01$). Pathological lymph node involvement was observed in only one patient (2%) of the solitary type. No significant differences were observed in lymphovascular invasion between the two types. EGFR mutations were negative in all patients. KRAS mutations were found in 23 (61%) of the solitary type and in 24 (75%) of the pneumonic type ($p = 0.22$), and TP53 mutations were found in four (11%) of the solitary type and in three (9%) of the pneumonic type ($p = 1$). BRAF, GNAS, ERBB2, and MET mutations and NRG1 fusions were rare. Expression of MUC1 was significantly higher in the pneumonic type than the solitary type ($p = 0.01$), while diffuse MUC6 positive expression was more frequent in the solitary type than the pneumonic type ($p = 0.02$).

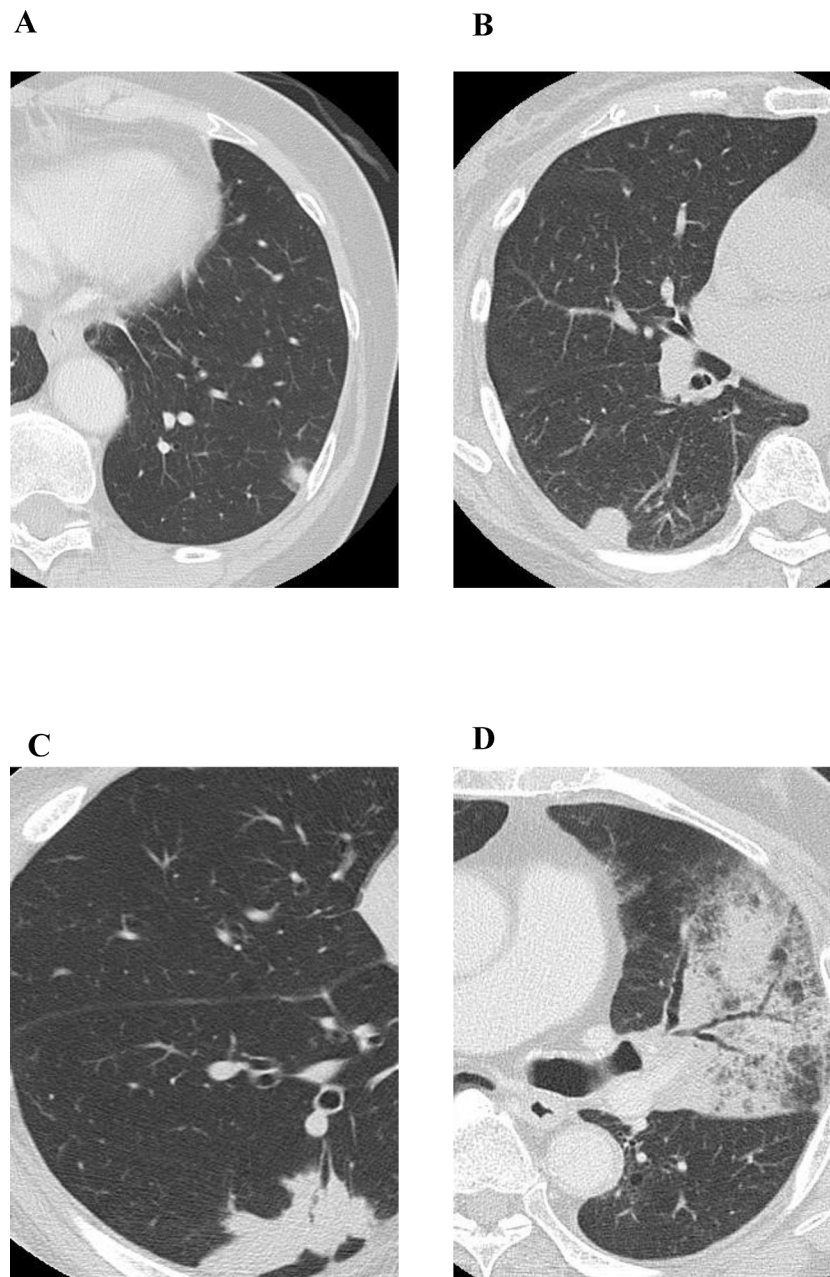


Fig. 1. Representative CT scan of invasive mucinous adenocarcinoma (IMA). A) Solitary type with ground-glass opacity (GGO). Solitary nodule showing a round shape with surrounding GGO. B) Solitary type without GGO. Solitary pure solid nodule showing a round shape. C) Pneumonic type without crazy-paving appearance (CPA). Consolidation showing an irregular margin. D) Pneumonic type with CPA. Consolidation showing an irregular margin with CPA.

3.3. Surgical outcomes of solitary type and pneumonic type IMA

Relapse site and cause of death are summarized in [Table 2](#). Four patients (11%) in the solitary type and 11 (34%) in the pneumonic type developed postoperative relapse ($p = 0.02$). In all patients, the site of relapse was the lung. One patient simultaneously developed distant metastasis. Lymph node metastasis was not observed in any patients. Causes of death were quite different between the two types. In the solitary type, only one patient died due to lung cancer, and four died due to other causes. In contrast, 12 patients died due to lung cancer, and two died due to other causes in the pneumonic type.

3.4. Clinical and biological characteristics of solitary type IMA according to the presence of GGO

The comparison of the clinical and biological characteristics of solitary type IMA according to the presence of GGO is shown in [Supplemental Table 1](#). SUVmax of tumors in the solitary type without GGO was significantly higher than that of the solitary type with GGO ($p = 0.04$). There was no significant difference in patient characteristics such as age, sex, smoking status, surgical mode, and clinicopathological stage. Significant differences were not observed in genetic alternations and mucin expression patterns.

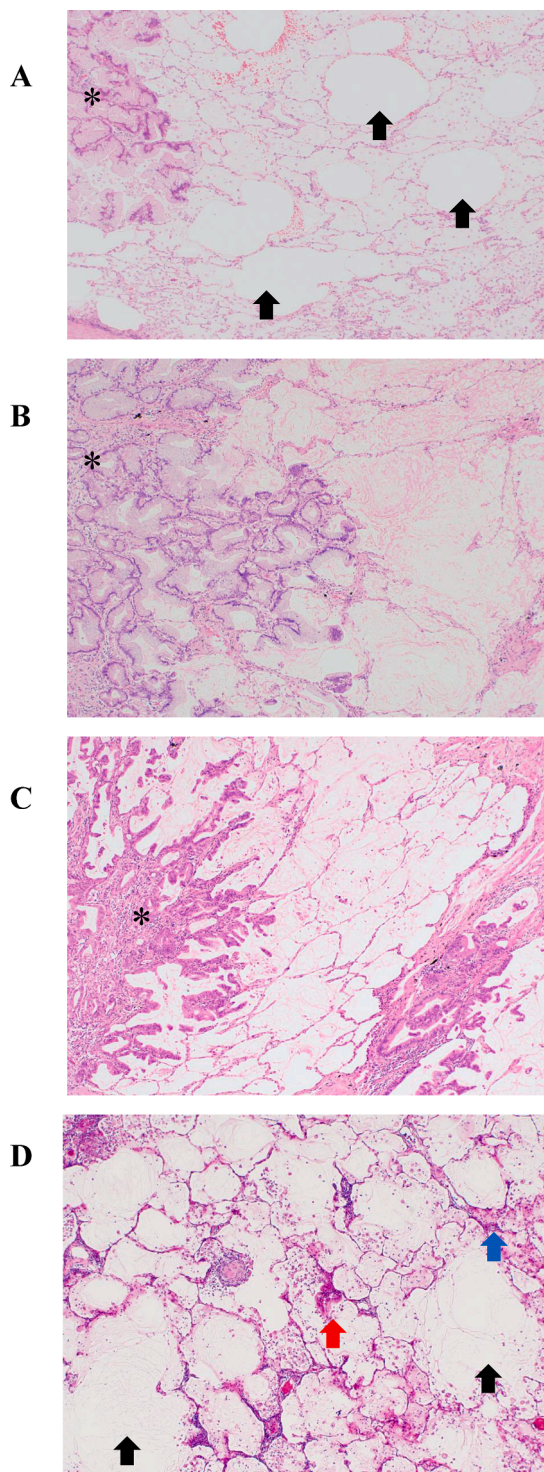


Fig. 2. Representative H&E staining of IMA in low-power view. A) Solitary type with GGO. The tumor region (*) is surrounded by intra-alveolar air space filled with mucin and the remaining intra-alveolar air space (black arrows), which was suspected to correspond to GGO. B) Solitary type without GGO. The tumor region (*) is surrounded by intra-alveolar air space filled with mucin. C) Pneumonic type without CPA. The pneumonic type without CPA and the solitary type without GGO were histologically indistinguishable. Neither type had any remaining intra-alveolar air space. D) Pneumonic type with CPA. The CPA area on CT was suspected to correspond to the area including the intra-alveolar air space filled with mucin (black arrows), infiltration of inflammatory cells into the intra-alveolar air space and interstitium, such as alveolar and interlobular septa (blue arrow), or lepidic and skipping tumor cell growth (red arrow) histologically.

3.5. Clinical and biological characteristics of pneumonic type IMA according to the presence of CPA

The comparison of clinical and biological characteristics of pneumonic type IMA according to the presence of CPA is shown in [Supplemental Table 2](#). Advanced clinicopathological stage and elevated serum CEA level were more common in pneumonic type with CPA than pneumonic type without CPA. Radiological tumor size of pneumonic type with CPA was larger than that of pneumonic type without CPA ($p < 0.01$), and the SUVmax of the tumor in the pneumonic type with CPA was significantly higher than that without CPA ($p = 0.04$). Significant differences were not observed in genetic alternations and mucin expression patterns.

3.6. Correlation between prognosis and radiological findings

The median follow-up time was 60 months. The 5-year OS rates were 82.2% and 62.8% in solitary type and pneumonic type IMA, respectively. Significant differences in OS were observed between the two types ($p = 0.02$; [Fig. 3A](#)). Survival curves for OS in four types were shown in [Fig. 3B](#). Solitary type with GGO had the best prognosis (5-year OS rate: 95.8%), and pneumonic type with CPA had the poorest prognosis (5-year OS rate: 50.0%). OS was better in the solitary type with GGO compared to that without GGO, however, the difference was not statistically significant ($p = 0.06$). There was no difference in OS between pneumonic types with and without CPA ($p = 0.24$). The 5-year RFS rates were 80.1% in solitary type and 50.2% in pneumonic type IMA. A significant difference in RFS was observed between two types ($p < 0.01$; [Fig. 3C](#)). Survival curves for RFS in four types were shown in [Fig. 3D](#). Solitary type with GGO had the best prognosis (5-year RFS rate: 86.6%), and pneumonic type with CPA had the poorest prognosis (5-year RFS rate: 28.6%). Although a significant difference in RFS was not observed between the solitary type with or without GGO ($p = 0.31$), a significant difference in RFS was observed between the pneumonic type with or without CPA ($p = 0.02$).

3.7. Histogram of the distribution of radiological characteristics

The histogram of the distribution of total size and SUVmax is shown in [Supplemental Fig. 1A, 1B](#). Tumors larger than 60 mm were observed only in pneumonic type with CPA ([Supplemental Fig. 1A](#)). Tumors with SUVmax higher than 10 were observed only in pneumonic type with CPA ([Supplemental Fig. 1B](#)).

4. Discussion

To our knowledge, this is the first report about the relationships between radiological characteristics and biological features, including pathological findings, gene alternations, and mucin expression in IMA. In the current study, we found that gene alternations of IMA have no difference between solitary type and pneumonic type IMA, and in terms of mucin expression pattern, solitary type tends to express MUC6, while pneumonic type tends to express MUC1.

There were differences in radiological characteristics between solitary type and pneumonic type IMA. The total size of tumor was larger in the pneumonic type than the solitary type, and SUVmax of tumor was higher in pneumonic type. In contrast, there was no difference in frequencies of driver oncogene alternations, including EGFR and KRAS mutations. These findings suggest that the two types of IMA may have the same development process. In addition, the solitary type without GGO showed higher SUVmax than the solitary type with GGO, and the pneumonic type with CPA showed larger tumor size and higher SUVmax than the pneumonic type without CPA. These findings suggest a stepwise progression of IMA in the following order: solitary type with GGO, solitary type without GGO, pneumonic type without CPA, and pneumonic type with CPA. Regarding immunohistochemistry, the expression of

Table 1
Comparison of clinical and biological characteristics between solitary type IMA and pneumonic type IMA.

		Solitary type (N = 38)		Pneumonic type (N = 32)		p value
Age	Median (range)	70	(44–83)	74	(41–85)	0.42
Sex	Male (%)	23	(61)	18	(57)	0.81
Pack year smoking	Median (range)	7.0	(0–126)	23.0	(0–104)	0.69
CEA positive	No. (%)	2	(5)	5	(15)	0.23
Clinical-stage	No. (%)					<0.01*
I		38	(100)	15	(47)	
II		0	(0)	14	(43)	
III		0	(0)	2	(6)	
IV		0	(0)	1	(3)	
Surgical mode	No. (%)					0.12**
WWR		6	(16)	1	(3)	
Segmentectomy		4	(11)	2	(6)	
Lobectomy		28	(74)	29	(90)	
Lymph node dissection	No. (%)					0.14
ND0		7	(18)	1	(3)	
ND1		8	(21)	7	(22)	
ND2		23	(61)	24	(75)	
Pathological-stage	No. (%)					<0.01***
I		25	(66)	17	(53)	
II		2	(5)	9	(28)	
III		1	(3)	6	(19)	
IV		0	(0)	2	(6)	
Total size on CT scan (mm)	Median (range)	16.5	(8–44)	48.0	(15–174)	<0.01
With GGO	Presence (%)	24	(63)	23	(72)	0.46
Multiple lesion	Presence (%)	2	(5)	3	(9)	0.65
SUVmax of tumor	Median (range)	1.6	(0–7.4)	4.9	(0–51)	<0.01
Pathological tumor size (mm)	Median (range)	15.0	(4–55)	41.5	(10–215)	<0.01
Lymph nodes metastasis	No. (%)	1	(3)	0	(0)	1
Lymphatic invasion	No. (%)	1	(3)	3	(9)	0.33
Vessel invasion	No. (%)	0	(0)	3	(9)	0.09
EGFR mutation	No. (%)	0	(0)	0	(0)	1
KRAS mutation	No. (%)	23	(61)	24	(75)	0.22
BRAF mutation	No. (%)	1	(3)	1	(3)	1
GNAS mutation	No. (%)	1	(3)	1	(3)	1
ERBB2 mutation	No. (%)	2	(5)	1	(3)	1
TP53 mutation	No. (%)	4	(11)	3	(9)	1
NRG1 fusion	No. (%)	1	(3)	0	(0)	1
MET mutation	No. (%)	1	(3)	0	(0)	1
MUC1 expression	Median (range)	5.0	(0–100)	20.0	(0–100)	0.01
MUC1 positive	No. (%)	18	(47)	23	(72)	0.052
MUC4 expression	Median (range)	4.0	(0–100)	5.0	(0–50)	0.83
MUC4 positive	No. (%)	12	(32)	11	(34)	1
MUC5AC expression	Median (range)	90.0	(3–100)	90.0	(70–100)	0.84
MUC5AC diffuse positive	No. (%)	25	(66)	26	(81)	0.18
MUC6 expression	Median (range)	70.0	(0–100)	25.5	(1–100)	0.06
MUC6 diffuse positive	No. (%)	15	(39)	4	(13)	0.02

WWR: Wide wedge resection.

CTR: Consolidation tumor ratio, GGO: Ground glass opacity, CPA: Crazy-paving appearance, SUV: Standard uptake value.

CEA positive: Elevated Serum CEA level > 5.0.

MUC1 positive: Expression of MUC1 \geq 10% of tumor cells.

MUC4 positive: Expression of MUC4 \geq 10% of tumor cells.

MUC5AC diffuse positive: Expression of MUC6 \geq 90% of tumor cells.

MUC6 diffuse positive: Expression of MUC6 \geq 90% of tumor cells.

ND0: No lymph node dissection.

ND1: Hilar lymph node dissection.

ND2: Mediastinal lymph node dissection.

* Clinical-stage: I versus II–IV.

** Surgical mode: Lobectomy versus sublobar resection.

*** Pathological-stage: I versus II–IV.

MUC1 was found to be more common in the pneumonic type, while expression of MUC6 was found to be more common in the solitary type. Genetically, MUC1 has been considered to be deeply involved in cancer growth and metastasis due to its association with proliferation signals in cancer cells or its inhibitory effects on intercellular adhesion and cell-substrate adhesion [20,21]. It has been reported that MUC1 expression correlates with a poor prognosis in non-small cell lung cancer [20,21]. In contrast, MUC6 is not expressed in normal lung tissue [22] and the specific mechanisms of production and function of MUC6 in IMA remain unclear. We previously reported that IMA showing MUC6 diffuse

expression was a distinct clinicopathological subset and less aggressive than IMA showing MUC6 patchy or negative expression. In the present study, MUC6 diffuse positive cases were more frequent in the solitary type than in the pneumonic type. However, our results also suggest that solitary and pneumonic type IMAs may have the same genetic origin. There is a contradiction in that solitary and pneumonic IMA have the same genetic origin but not the same mucin phenotype. A possible explanation for this discrepancy is that solitary type IMA with diffuse MUC6 expression may be an early lesion of IMA, and MUC6 expression decreases in accordance with the stepwise progression from solitary to

Table 2
Relapse site and cause of death in solitary type and pneumonic type IMA.

Relapse Site	No. (%)	Solitary type (N = 38)		Pneumonic type (N = 32)		p value
		No.	(%)	No.	(%)	
Staple line	4	1	(3)	0	(0)	0.02
Ipsilateral lung	2	2	(5)	5	(16)	
Contralateral lung	1	1	(3)	9	(28)	
Lymph node	0	0	(0)	0	(0)	
Liver	1	1	(3)	0	(0)	
Death	No. (%)	5	(13)	14	(43)	<0.01
Lung cancer	1	1	(3)	12	(38)	
Other cause						
Aortic dissection	1	1	(3)	0	(0)	
Pneumonia	2	2	(5)	1	(3)	
Stroke	1	1	(3)	0	(0)	
Unknown	0	0	(0)	1	(3)	

pneumonic type IMA. In other organs such as bile tract cancer and pancreatic cancer, MUC6 expression is decreased in invasive adenocarcinomas compared to in situ neoplasms, signaling the acquisition of malignancy [23–25]. Furthermore, in vitro studies, MUC6 expression cells showed significantly lower proliferation, motility, and invasiveness than control cells [9,26]. In contrast, MUC1 may increase if the biological grade of the malignancy becomes higher.

GGO was defined as the focal nodular areas of increased lung attenuation, through which normal parenchymal structures, including airways and vessels, could be visualized [27]. Histologically, the tumor region was surrounded by intra-alveolar air space filled with mucin and the remaining intra-alveolar air space in the solitary type with GGO, while it was surrounded by intra-alveolar air space filled with mucin in solitary type without GGO. Based on these histological differences, the GGO component observed on CT was suspected to correspond to the remaining intra-alveolar air space. These findings suggest that the air space surrounding the tumor is gradually filled with mucin with tumor growth. CPA has a variety of causes, including infectious, neoplastic, idiopathic, inhalational, and sanguineous disorders [15,16]. In general,

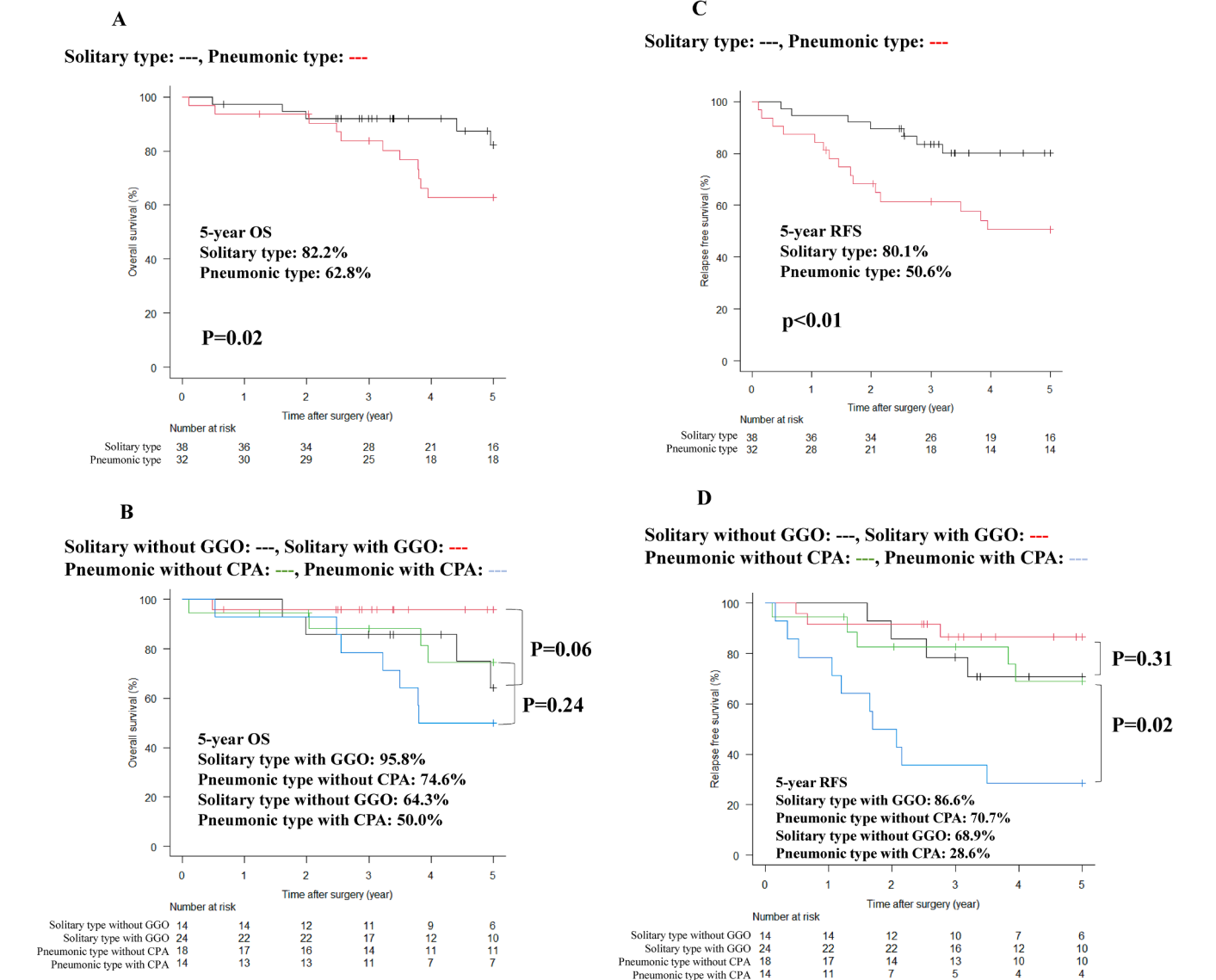


Fig. 3. Kaplan-Meier curves of 5-year overall survival (OS) and 5-year relapse free survival (RFS) for patients with IMA. A) 5-year OS in Solitary type and pneumonic type. B) 5-year OS in Solitary type with or without GGO and pneumonic type with or without CPA. C) 5-year RFS in Solitary type and pneumonic type. D) 5-year RFS in Solitary type with or without GGO and pneumonic type with or without CPA.

the radiological feature of CPA reflects the thickened interlobular septa or interstitium and material fills within the alveoli. In IMA, the CPA area on CT was suspected to correspond to the area including the intra-alveolar air space filled with mucin, infiltration of the interstitium by inflammatory cells or lepidic and skipping tumor cell growth histologically.

PET-CT is useful to predict relapse in lung cancer, and high SUVmax is correlated with invasive tumors [28,29]. In terms of IMA, tumors containing large amounts of mucus tend to have low FDG accumulation, and FDG accumulation in IMA is often lower than that in other types of lung adenocarcinomas [30]. However, we found that SUVmax was frequently high value in pneumonic type with CPA. Pneumonic type with CPA may get a biological malignancy grade while a tumor increases.

There were some limitations in this study. First, this study was based on a single-institution Japanese database, and the number of cases is relatively small (N = 70). Second, this study was a retrospective observational study about IMA that diagnosed only surgically resected patients. Because of its retrospective nature, there was a bias in the selection of the surgical mode, and there were no patients with poor performance status or difficulty to treat medically.

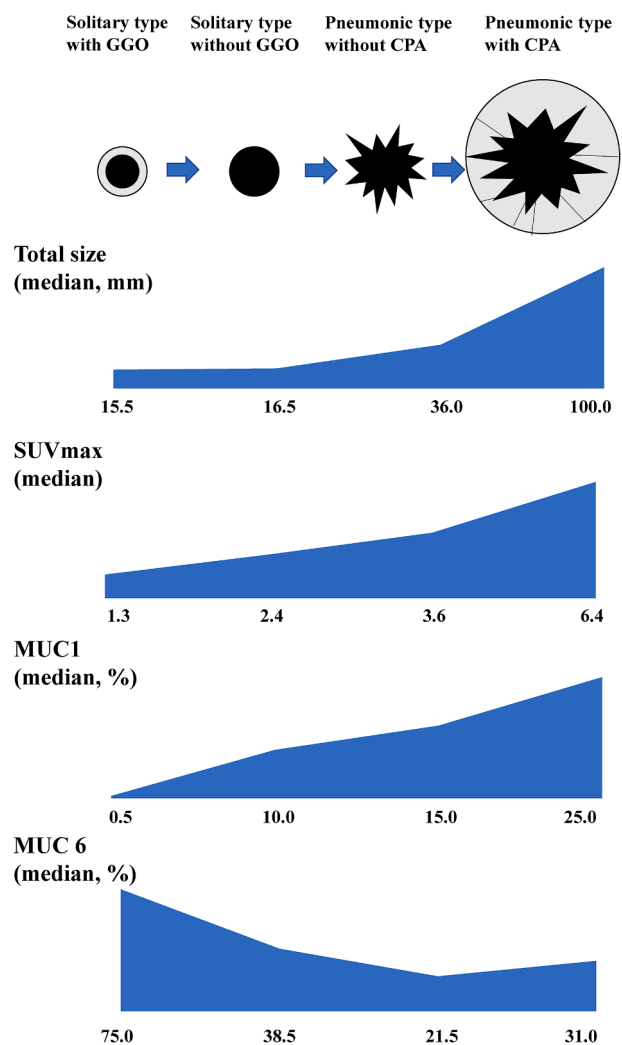


Fig. 4. Stepwise progression of 4 types of IMA, and differences of total size, SUVmax, MUC1, and MUC6.

5. Conclusions

Solitary type and pneumonic type IMA may be genetically of the same origin. Stepwise progression of IMA, in order to solitary type with GGO, solitary type without GGO, pneumonic type without CPA, and pneumonic type with CPA, was suggested based on tumor size, SUVmax, MUC1 and MUC6 expression patterns, and prognosis (Fig. 4).

CRedit authorship contribution statement

Eisuke Goto: Conceptualization, Methodology, Formal analysis, Investigation, Resources, Writing – original draft. **Kazuya Takamochi:** Methodology, Investigation, Formal analysis, Writing – review & editing. **Satsuki Kishikawa:** Visualization, Investigation, Resources, Funding acquisition. **Takuo Hayashi:** Visualization, Resources, Investigation. **Takuya Ueda:** Data curation, Writing – original draft. **Aritoshi Hattori:** Writing – review & editing. **Mariko Fukui:** Writing – review & editing. **Takeshi Matsunaga:** Writing – review & editing. **Kenji Suzuki:** Writing – review & editing, Supervision.

Declaration of Competing Interest

The authors declare that they have no known competing financial interests or personal relationships that could have appeared to influence the work reported in this paper.

Acknowledgements

This work was carried out in part at the Intractable Disease Research Center, Juntendo University, and supported by the Grant-in-Aid for Japan Society for the Promotion of Science (JSPS) KAKENHI (grant numbers 18K15095, 19K07469) and the Practical Research for Innovative Cancer Control (grant number JP18ck0106252) from the Japan Agency for Medical Research and Development, AMED. This work was also supported in part by the Takeda Science Foundation, the Smoking Research Foundation, and the Project for Research from Environmental and Gender-Specific Medicine (grant number E2824).

Appendix A. Supplementary material

Supplementary data to this article can be found online at <https://doi.org/10.1016/j.lungcan.2023.107348>.

References

- [1] W.D. Travis, E. Brambilla, A.G. Nicholson, Y. Yatabe, J.H.M. Austin, M.B. Beasley, L.R. Chirieac, S. Dacic, E. Duhig, D.B. Flieder, K. Geisinger, F.R. Hirsch, Y. Ishikawa, K.M. Kerr, M. Noguchi, G. Pelosi, C.A. Powell, M.S. Tsao, I. Wistuba, World Health Organization classification of lung tumors: impact of genetic, clinical and radiologic advances since the 2004 classification, *J. Thorac. Oncol.* 10 (9) (2015) 1243–1260.
- [2] W.D. Travis, E. Brambilla, M. Noguchi, A.G. Nicholson, K.R. Geisinger, Y. Yatabe, D.G. Beer, C.A. Powell, G.J. Riely, P.E. Van Schil, K. Garg, J.H. Austin, H. Asamura, V.W. Rusch, F.R. Hirsch, G. Scagliotti, T. Mitsudomi, R.M. Huber, Y. Ishikawa, J. Jett, M. Sanchez-Cespedes, J.P. Sculier, T. Takahashi, M. Tsuboi, J. Vansteenkiste, I. Wistuba, P.C. Yang, D. Aberle, C. Brambilla, D. Flieder, W. Franklin, A. Gazdar, M. Gould, P. Hasleton, D. Henderson, B. Johnson, D. Johnson, K. Kerr, K. Kuriyama, J.S. Lee, V.A. Miller, I. Petersen, V. Roggli, R. Rosell, N. Saijo, E. Thunnissen, M. Tsao, D. Yankelewitz, International Association for the Study of Lung Cancer/American Thoracic Society/European Respiratory Society international multidisciplinary classification of lung adenocarcinoma, *J. Thorac. Oncol.* 6 (2011) 244–285, <https://doi.org/10.1097/JTO.0b013e318206a221>.
- [3] WHO Classification of Tumors. Thoracic Tumors Vol. 5, 5th edition (IARC, 2021).
- [4] A. Warth, T. Muley, M. Meister, A. Stenzinger, M. Thomas, P. Schirmacher, P. A. Schnabel, J. Budczies, H. Hoffmann, W. Weichert, The novel histologic International Association for the Study of Lung Cancer/American Thoracic Society/European Respiratory Society classification system of lung adenocarcinoma is a stage-independent predictor of survival, *J. Clin. Oncol.* 30 (2012) 1438–1446, <https://doi.org/10.1200/JCO.2011.37.2185>.
- [5] H.S. Shim, M. Kenudson, Z. Zheng, M. Liebers, Y.J. Cha, Q. Hoang Ho, M. Onozato, L. Phi Le, R.S. Heist, A.J. Iafrate, Unique genetic and survival characteristics of

- invasive mucinous adenocarcinoma of the lung, *J. Thorac. Oncol.* 10 (2015) 1156–1162, <https://doi.org/10.1097/JTO.0000000000000579>.
- [6] K. Kadota, Y.C. Yeh, S.P. D'Angelo, A.L. Moreira, D. Kuk, C.S. Sima, G.J. Riely, M. E. Arcila, M.G. Kris, V.W. Rusch, P.S. Adusumilli, W.D. Travis, Associations between mutations and histologic patterns of mucin in lung adenocarcinoma: invasive mucinous pattern and extracellular mucin are associated with KRAS mutation, *Am. J. Surg. Pathol.* 38 (2014) 1118–1127, <https://doi.org/10.1097/PAS.0000000000000246>.
- [7] C. Casali, G. Rossi, A. Marchioni, G. Sartori, F. Maselli, L. Longo, E. Tallarico, U. Morandi, A single institution-based retrospective study of surgically treated bronchioloalveolar adenocarcinoma of the lung: clinicopathologic analysis, molecular features, and possible pitfalls in routine practice, *J. Thorac. Oncol.* 5 (2010) 830–836, <https://doi.org/10.1097/jto.0b013e3181d60ff5>.
- [8] S. Kishikawa, T. Hayashi, T. Saito, K. Takamochi, S. Kohsaka, K. Sano, N. Sasahara, K. Sasa, T. Kurihara, K. Hara, Y. Suehara, F. Takahashi, K. Suzuki, T. Yao, Diffuse expression of MUC6 defines a distinct clinicopathological subset of pulmonary invasive mucinous adenocarcinoma, *Mod. Pathol.* 34 (2021) 786–797, <https://doi.org/10.1038/s41379-020-00690-w>.
- [9] K. Yamanoi, C. Fujii, H. Yuzuriha, M. Kumazawa, M. Shimoda, K. Emoto, H. Asamura, J. Nakayama, MUC6 expression is a preferable prognostic marker for invasive mucinous adenocarcinoma of the lung, *Histochem. Cell Biol.* 157 (2022) 671–684, <https://doi.org/10.1007/s00418-022-02093-1>.
- [10] H. Watanabe, H. Saito, T. Yokose, Y. Sakuma, S. Murakami, T. Kondo, F. Oshita, H. Ito, H. Nakayama, K. Yamada, M. Iwazaki, Relation between thin-section computed tomography and clinical findings of mucinous adenocarcinoma, *Ann. Thorac. Surg.* 99 (2015) 975–981, <https://doi.org/10.1016/j.athoracsur.2014.10.065>.
- [11] T. Wang, Y. Yang, X. Liu, J. Deng, J. Wu, L. Hou, C. Wu, Y. She, X. Sun, D. Xie, C. Chen, Primary invasive mucinous adenocarcinoma of the lung: prognostic value of CT imaging features combined with clinical factors, *Korean J. Radiol.* 22 (2021) 652–662, <https://doi.org/10.3348/kjr.2020.0454>.
- [12] H.Y. Lee, M.J. Cha, K.S. Lee, H.Y. Lee, O.J. Kwon, J.Y. Choi, H.K. Kim, Y.S. Choi, J. Kim, Y.M. Shim, Prognosis in resected invasive mucinous adenocarcinomas of the lung: related factors and comparison with resected nonmucinous adenocarcinomas, *J. Thorac. Oncol.* 11 (2016) 1064–1073, <https://doi.org/10.1016/j.jtho.2016.03.011>.
- [13] T. Matsui, N. Sakakura, S. Koyama, K. Nakanishi, E. Sasaki, S. Kato, W. Hosoda, Y. Murakami, H. Kuroda, Y. Yatabe, Comparison of surgical outcomes between invasive mucinous and non-mucinous lung adenocarcinoma, *Ann. Thorac. Surg.* 112 (2021) 1118–1126, <https://doi.org/10.1016/j.athoracsur.2020.09.042>.
- [14] K.S. Beck, Y.E. Sung, K.Y. Lee, D.H. Han, Invasive mucinous adenocarcinoma of the lung: serial CT findings, clinical features, and treatment and survival outcomes, *Thorac. Cancer* 11 (2020) 3463–3472, <https://doi.org/10.1111/1759-7714.13674>.
- [15] W. De Wever, J. Meerschaert, J. Coolen, E. Verbeken, J.A. Verschakelen, The crazy-paving pattern: a radiological-pathological correlation, *Insights Imaging* 2 (2011) 117–132, <https://doi.org/10.1007/s13244-010-0060-5>.
- [16] S.E. Rossi, J.J. Erasmus, M. Volpacchio, T. Franquet, T. Castiglioni, H.P. McAdams, “Crazy-paving” pattern at thin-section CT of the lungs: radiologic-pathologic overview, *Radiographics* 23 (2003) 1509–1519, <https://doi.org/10.1503/cmaj.091422>.
- [17] K. Takamochi, F. Takahashi, Y. Suehara, E. Sato, S. Kohsaka, T. Hayashi, S. Kitano, T. Ueno, S. Kojima, K. Takeuchi, H. Mano, K. Suzuki, DNA mismatch repair deficiency in surgically resected lung adenocarcinoma: Microsatellite instability analysis using the Promega panel, *Lung Cancer* 8 (110) (2017) 26–31, <https://doi.org/10.1016/j.lungcan.2017.05.016>.
- [18] K. Hara, T. Saito, T. Hayashi, A. Yimit, M. Takahashi, K. Mitani, M. Takahashi, T. Yao, A mutation spectrum that includes GNAS, KRAS and TP53 may be shared by mucinous neoplasms of the appendix, *Pathol. Res. Pract.* 211 (9) (2015) 657–664, <https://doi.org/10.1016/j.prp.2015.06.004>.
- [19] S. Kohsaka, T. Hayashi, M. Nagano, T. Ueno, S. Kojima, M. Kawazu, Y. Shiraishi, S. Kishikawa, Y. Suehara, F. Takahashi, K. Takahashi, K. Suzuki, K. Takamochi, H. Mano, Identification of Novel CD74-NRG2 α Fusion From Comprehensive Profiling of Lung Adenocarcinoma in Japanese Never or Light Smokers, *J. Thorac. Oncol.* 15 (6) (2020 Jun) 948–961, <https://doi.org/10.1016/j.jtho.2020.01.021> (Epub 2020 Feb 6 PMID: 32036070).
- [20] F. Guddo, A. Giatromanolaki, C. Patriarca, J. Hilken, C. Reina, R.M. Alfano, A. M. Vignola, M.I. Koukourakis, M. Gambacorta, G. Pruneri, G. Coggi, G. Bonsignore, Depolarized expression of episialin (EMA, MUC1) in lung adenocarcinoma is associated with tumor progression, *Anticancer Res.* 18 (1998) 1915–1920.
- [21] M. Woenckhaus, J. Merk, R. Stoehr, F. Schaeper, A. Gaumann, K. Wiebe, A. Hartmann, F. Hofstaedter, W. Dietmaier, Prognostic value of FHIT, CTNNB1, and MUC1 expression in non-small cell lung cancer, *Hum. Pathol.* 39 (2008) 126–136, <https://doi.org/10.1016/j.humpath.2007.05.027>.
- [22] C.J. Reid, S. Gould, A. Harris, Developmental expression of mucin genes in the human respiratory tract, *Am. J. Respir. Cell Mol. Biol.* 17 (1997) 592–598, <https://doi.org/10.1165/ajrcmb.17.5.2798>.
- [23] A. Ohya, K. Yamanoi, H. Shimojo, C. Fujii, J. Nakayama, Gastric gland mucin-specific O-glycan expression decreases with tumor progression from precursor lesions to pancreatic cancer, *Cancer Sci.* 108 (2017) 1897–1902, <https://doi.org/10.1111/cas.13317>.
- [24] K. Yamanoi, K. Ishii, M. Tsukamoto, S. Asaka, J. Nakayama, Gastric gland mucin-specific O-glycan expression decreases as tumor cells progress from lobular endocervical gland hyperplasia to cervical mucinous carcinoma, gastric type, *Virchows Arch.* 473 (2018) 305–311, <https://doi.org/10.1267/ahc.21-00032>.
- [25] M. Okumura, K. Yamanoi, T. Uehara, J. Nakayama, Decreased alpha-1,4-linked N-acetylglucosamine glycosylation in biliary tract cancer progression from biliary intraepithelial neoplasia to invasive adenocarcinoma, *Cancer Sci.* 111 (2020) 4629–4635, <https://doi.org/10.1111/cas.14677>.
- [26] A. Yuki, C. Fujii, K. Yamanoi, H. Matoba, S. Harumiya, M. Kawakubo, J. Nakayama, Glycosylation of MUC6 by α 1,4-linked N-acetylglucosamine enhances suppression of pancreatic cancer malignancy, *Cancer Sci.* 113 (2022) 576–586, <https://doi.org/10.1111/cas.15209>.
- [27] D.M. Hansell, A.A. Bankier, H. MacMahon, T.C. McLoud, N.L. Müller, J. Remy, Fleischner Society: glossary of terms for thoracic imaging, *Radiology* 246 (2008) 697–722, <https://doi.org/10.1148/radiol.2462070712>.
- [28] H.Y. Lee, S.W. Lee, K.S. Lee, J.Y. Jeong, J.Y. Choi, O.J. Kwon, S.H. Song, E.Y. Kim, J. Kim, Y.M. Shim, Role of CT and PET Imaging in Predicting Tumor Recurrence and Survival in Patients with Lung Adenocarcinoma: A Comparison with the International Association for the Study of Lung Cancer/American Thoracic Society/European Respiratory Society Classification of Lung Adenocarcinoma, *J. Thorac. Oncol.* 10 (2015) 1785–1794, <https://doi.org/10.1097/JTO.0000000000000689>.
- [29] S. Iwano, M. Kishimoto, S. Ito, K. Kato, R. Ito, S. Naganawa, Prediction of pathologic prognostic factors in patients with lung adenocarcinomas: comparison of thin-section computed tomography and positron emission tomography/computed tomography, *Cancer Imaging* 22 (14) (2014) 3, <https://doi.org/10.1186/1470-7330-14-3>.
- [30] H. Nakamura, H. Saji, T. Shinmyo, R. Tagaya, N. Kurimoto, H. Koizumi, M. Takagi, Close association of IASLC/ATS/ERS lung adenocarcinoma subtypes with glucose-uptake in positron emission tomography, *Lung Cancer* 87 (2015) 28–33, <https://doi.org/10.1016/j.lungcan.2014.11.010>.